33RD CONGRESS
OF THE INTERNATIONAL COUNCIL
OF THE AERONAUTICAL SCIENCES
STOCKHOLM, SWEDEN, 4-9 SEPTEMBER, 2022

ICAS 2022 SWEDEN

AIRFOIL DESIGN BY MULTI-ADDITIONAL SAMPLING MULTI-FIDELITY EFFICIENT GLOBAL OPTIMIZATION

Krittin Khankwa[1], Tharathep Phiboon[1], Atthaphon Ariyarit[1], Rattaporn Kasemsri[2] & Masahiro Kanazaki[3]

[1]School of Mechanical Engineering, Institute of Engineering, Suranaree University of Technology, 111, MahaWitthayalai Rd, Suranaree, Mueang Nakhon Ratchasima District, Nakhon Ratchasima 30000, Thailand
[2]School of Civil Engineering, Institute of Engineering, Suranaree University of Technology, 111, MahaWitthayalai Rd, Suranaree, Mueang Nakhon Ratchasima District, Nakhon Ratchasima 30000, Thailand
[3]Department of Aeronautics and Astronautics, Graduate School of System Design, Tokyo Metropolitan University, 6-6, Asahigaoka, Hino-Shi, Tokyo 191-0065, Japan

Abstract

An Efficient global optimization (EGO), with multi-additional sampling multi-fidelity for single-objective optimization via expected improvement (EI) process in genetic algorithm, is applied to reduce the time and computational cost for aerodynamic design. The generating fidelity data and the maximization EI are used for finding the additional sampling to improve the Kriging surrogate model during the EGO process. The objective of this research is to find NACA 4-digit optimal airfoil design with maximized proportion lift coefficient (C_l) to drag coefficient (C_d) at C_l = 0.5 with the condition at 1,000,000 of Reynolds number. The EGO evaluation and numerical method indicate the result of optimal airfoil design with NACA 4305 airfoil design and C_l/C_d is approximately 47.20 at an approximate 0.55 degree of angle of attack with a 2.08% C_l/C_d improvement compared with the maximum C_l/C_d of its initial sampling.

Keywords: Efficient Global Optimization, Computational Fluid Dynamics, Airfoil Design

1. Introduction

The wing is an important component for creating lift power in an aircraft as it moves through the air. The cross-section form of the wing, known as an "airfoil," splits the airflow to create a distinct pressure, which gives the advantage of generating lift force for an aircraft. The shape of the airfoil will affect the aerodynamic performance in terms of lift and drag; previously, the airfoil design process used actual experiments with airflow in wind tunnel tests, then measuring and observing the force that happens to the wing; however, wind tunnel tests are expensive to create, especially to construct the wing specimen which is scaled-down but remains the same geometrical wing shape. Another designing process, numerical and analysis design, apply aerodynamic theory to design optimum airfoil shape with the computer then collect the simulation data but this method also takes high cost for computation calculation and time.

To reduce experiment cost and computing time, Efficient global optimization (EGO) [6] with multi-additional sampling, multi-fidelity will be applied. Multi-additional sampling [2] via maximizing Expected Improvement (EI) value and multi-fidelity [2] via different data resources.

The EGO with multi-additional sampling and multiple objectives [9] was purposed to solve the airfoil aerodynamic design problem for minimizing drag and maximizing airfoil thickness at the trailing edge. Another study [7] improved multi-additional sampling via Expected Improvement (EI) for the EGO to test with test function and airfoil design problem.

In this research, An EGO with multi-additional sampling will be applied for solving a single objective aerodynamic airfoil design problem, with the goal of maximizing the proportion of lift coefficient (C_l) to drag coefficient (C_d).

2. Methodology

2.1 Multi-Additional Sampling Multi-Fidelity Single-Objective Efficient Global Optimization

The EGO [6] procedure displays here in Figure 1. The EGO algorithm based on the ordinary Kriging method, firstly, begins its operation by generating the high and low fidelity initial sampling for the design of the experiment via using the Latin Hypercube Sampling [5], or LHS. Then, evaluate the data sample and apply the Kriging method to create the Kriging surrogate model [8] to predict the function of sampling point. Finally, an additional sampling point is found by maximizing the Expected Improvement (EI) value using the genetic algorithms (GA) [1]. The definition of the EI at point (x) is given by

$$I(x) = max[f_{ref} - \hat{y}(x), 0] \tag{1}$$

$$E[I(x)] = \int_{\infty}^{f_{ref}} (f_{ref} - \hat{y}(x)) \times \phi(\hat{y}(x))dy \tag{2}$$

where ϕ stands for the probability density function representing uncertainty about $\hat{y}(x)$, which predicts a function value from a surrogate model. Additional sampling points, based on the calculation, are repeated until the objective function are converges.

High-fidelity data is the expensive data that is high accuracy but high time-consuming for calculation and has a lower quantity than low-fidelity data. Low-fidelity data is the inexpensive data that has less accuracy but more quantity and can be rapidly acquired from the calculation. Both fidelity data can be combined to use the advantage of each for generating a surrogate model.

The fidelity data in this research is implemented by numerical method via Computational Fluid Dynamics (CFD) from for the high-fidelity data and panel method theory for the low-fidelity data.

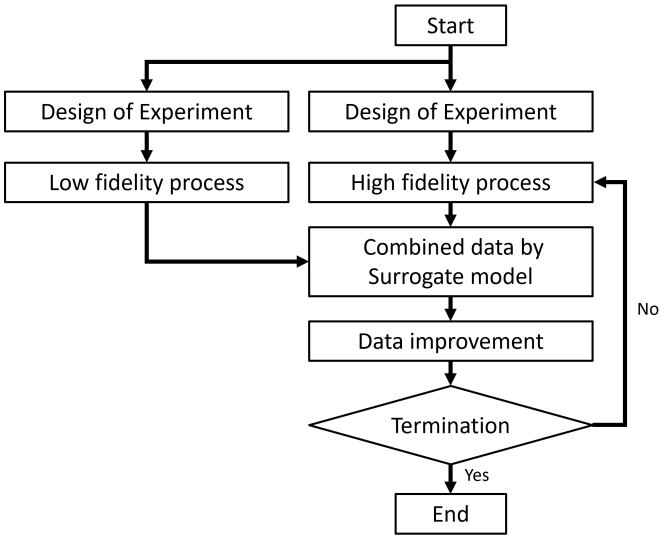

Figure 1 – Flowchart of Multi-Additional Sampling Multi-Fidelity EGO [2].

2.1.1 Low-fidelity data

Low-fidelity data in this study is Xfoil [3] software. As inexpensive data, it uses a high-order panel method and a fully-coupled viscous/inviscid interaction method to evaluate drag, boundary layer transition, and separation. The viscous analysis of Xfoil can be used to predict lift coefficient (C_l) and drag coefficient (C_d) [4]. The design variables from the design of experiment or LHS process are used to generate the shape of the airfoil to calculate the aerodynamics value with Xfoil. The panel quantity in this study is 300 panels with varying the angle of attack (AoA) between 0 to 15 degrees to acquire the required aerodynamic data. The experiment data of NACA 0012 [10] is used to validate the aerodynamic data accuracy and mesh independent of the computation.

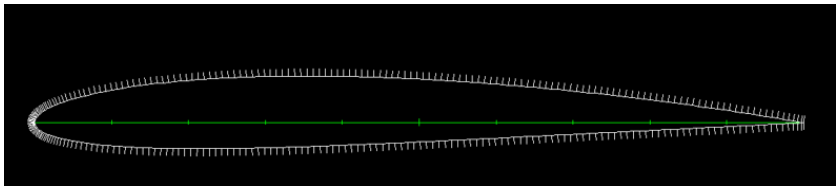

Figure 2 – Airfoil sample with panel setting for the Xfoil software.

2.1.2 High-fidelity data

High-fidelity data in this study is CFD FLUENT (ANSYS FLUENT) software with the viscous model as the Spalart-Allmaras turbulence model [11] to obtain the aerodynamic force that acts on the airfoil shape. C-type mesh is applied for the flow boundary with ten times larger than the chord length of the airfoil and the mesh element quantity is approximately 540,000 elements. The angle of attack is also varying between 0 to 15 degrees to acquire the required aerodynamic data.

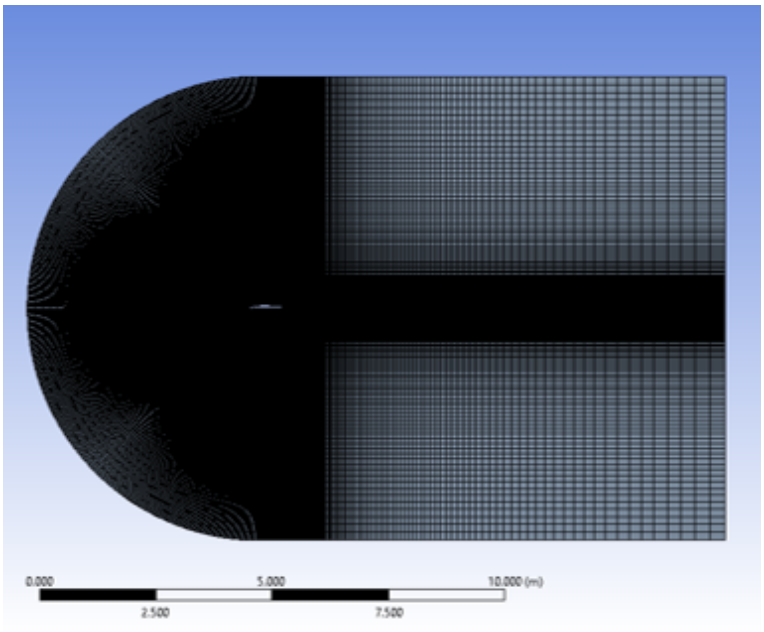

Figure 3 – C-type mesh for CFD FLUENT.

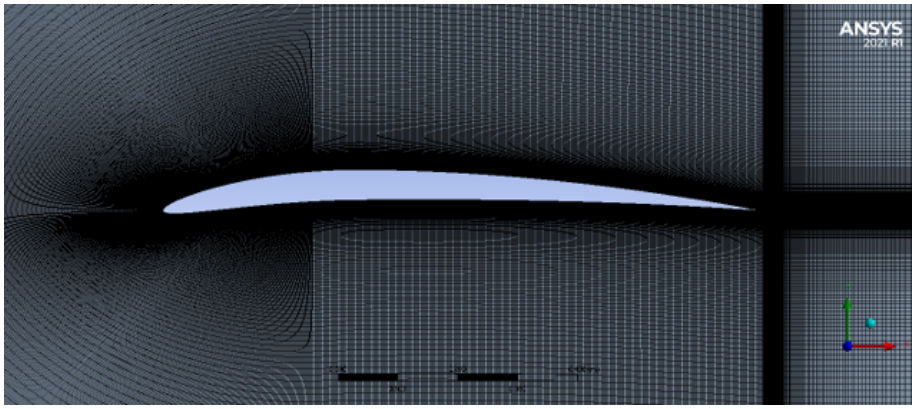

Figure 4 – Airfoil with mesh element inside C-type mesh.

2.1.3 Kriging method

An unknown function $\hat{y}(x)$ can be estimated by using a Kriging method [8] in the following equation:

$$\hat{y}(x) = \mu(x) - \varepsilon(x) \tag{3}$$

where $\hat{y}(x)$ designated as a global model and $\varepsilon(x)$ as a local model. An equation $\mu(x)$ is given by

$$\mu(x) = \frac{\mathbf{1}^{\mathbf{T}}\mathbf{R}^{-1}\mathbf{F}}{\mathbf{1}^{\mathbf{T}}\mathbf{R}^{-1}\mathbf{1}} \tag{4}$$

where $\mathbf{R}$ denotes a matrix of the correlation between the sample points, and $\mathbf{F}$ denotes a vector containing the evaluation data of each sampling point. The μ is set to a constant value for the global model, and $(\varepsilon(x))$ is the local model, that expressed as

$$\varepsilon(x) = r(x)^{-1}\mathbf{R}^{-1}(\mathbf{F} - \mathbf{1})\mu \tag{5}$$

where $r(x)$ denotes a vector written in terms of x.$r(x)$ denotes a vector of sampling points. The correlation value of $\varepsilon(x)$ and $\varepsilon(x^i)$ is a distance function between x and x^i. In the Kriging model, the local derivation at an unknown point x is predicted via stochastic processes.

Node 1	Node 2	Node 3	Node 4	...
Sampling				
Evaluation1	Evaluation2	Evaluation3	Evaluation4	
EI Maximization	Unused	Unused	Unused	...
Additional Evaluation1				
EI Maximization				
Additional Evaluation2				

Node 1	Node 2	Node 3	Node 4	...
Sampling				
Evaluation1	Evaluation2	Evaluation3	Evaluation4	
EI Maximization				
Additional Evaluation1	Additional Evaluation2	Additional Evaluation3	Additional Evaluation3	...
⋮	⋮	⋮	⋮	

Figure 5 – (a) Diagram of single computing EGO, (b) Diagram of parallel computing EGO [2].

2.1.4 Multiple Additional Sampling for Single-Objective Optimization

The EGO can achieve a single additional sample in each iteration but there is the limitation to the user that using computational resources can only use for a single evaluation, and the initial sampling can be created by parallel evaluation. The limitation continues during the additional sampling process and computational resources cannot be used (see Figure 5(a)). Moreover, for maintenance the diversity of additional samples in surrogate model's improvement via EI maximization, there require several iterations to achieve the additional sampling for optimization solving possible.

In this research, multi-additional sampling (MAs) for single-objective optimization is applied to solve three airfoil design problems, the sub-iteration is added to the EGO process (see Figure 5(b)). An acquired additional sample via iteration is added to update the surrogate model; by adopting the predicted point of $(x, \hat{y}(x))$ that represents a temporal function value. Then, the acquisition of one more additional sample using EI maximization is done.

Figure 6 shows a schematic diagram of an additional sampling process with MAs. The initial process starts with the acquisition of $x_{EI,max1}$ via EI maximization on the Kriging model and evaluation of the predicted value $\hat{y}_{a1}$ from $x_{EI,max1}$. Using $x_{EI,max1}, \hat{y}_{a1}$ generates a temporary model. EI maximizes $x_{EI,max1}$ to find another additional point as $x_{EI,max2}$ but $x_{EI,max1}$ should not be greater than $x_{EI,max2}$. Subsequently, the precise value of $y_{a1}, y_{a2}, \ldots$ can be obtained by calculation via parallel evaluation for $x_{EI,max1}, x_{EI,max2}, \ldots$.

Finally, the value from additional sampling has to be put in the data set to improve the model. In sub-iteration, there must be $\hat{y}(x)$ values whose prediction is done by the Kriging model. Therefore, multiple additional samples are able to obtain rapidly. In the main iteration, the precise value for additional samples can be calculated via parallel evaluation. Using the EGO method uses less design time than the original iteration.

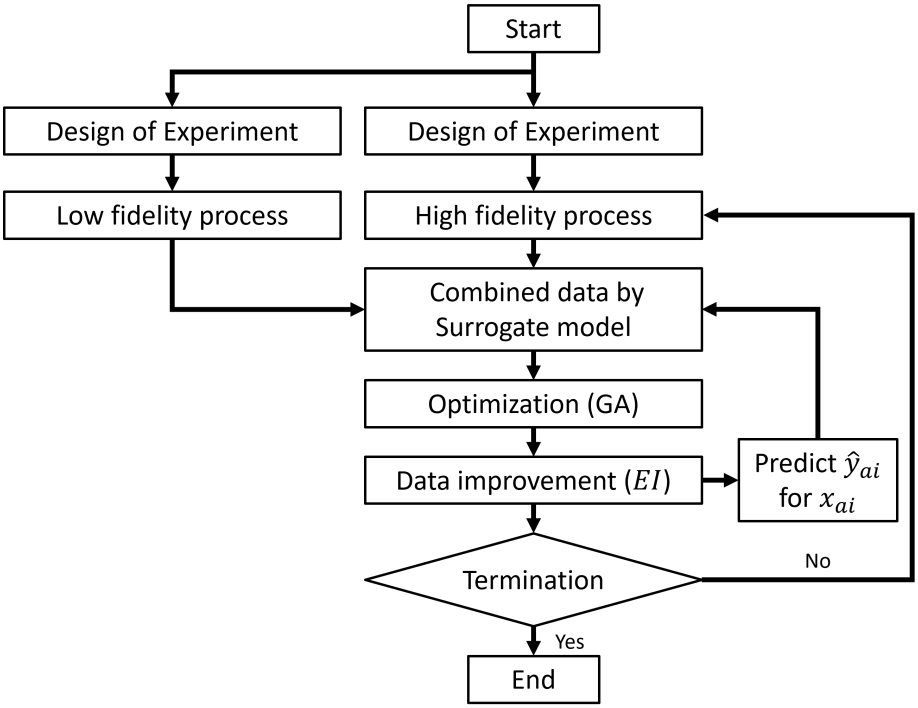

Figure 6 – Flowchart of parallel computing Multi-Additional Sampling Multi-Fidelity EGO [2].

3. Airfoil design problem

In this research, the objective for airfoil design is to maximize the proportion of lift coefficient (C_l) to drag coefficient (C_d) at Reynolds number at 1,000,000 with NACA 4-digit airfoil design variable. NACA 4-digit design variable range:

- Percent of maximum camber at 0% to 5% of chord length.
- Percent of maximum camber position at 10% to 50% of chord length.
- Percent of maximum airfoil thickness at 5% to 15% of chord length.
- Operate at Reynolds number at 1,000,000

Objective: Maximize $C_\mathrm{l}/C_\mathrm{d}$ at C_l = 0.5 The number of initial samplings is set to 10 and the number of additional samplings is set to 10. The number of additional sampling in each sub-iterations is set to 2, for example, two additional samples are acquired for evaluation in each main iteration. For aerodynamic evaluation, numerical methods such as the Computational Fluid Dynamics (CFD) method from CFD FLUENT as high-fidelity data and the higher panel method theory from Xfoil are both applied for evaluation in the specified condition.

4. Results and Discussion

4.1 Results

From the multi-additional sampling multi-fidelity EGO and aerodynamic evaluation, an acquired airfoil high-fidelity data in each sampling number of airfoils is shown in Table 1. From this table, the optimum design is found at sampling number 17 (the fourth iteration of optimization process) that can be obtained the maximum $C_l/C_d = 47.1985$. Figure 8 represents comparison between additional sampling from entire iterations and maximum C_l/C_d of its initial sampling at sampling number 8 with a percent of improvement maximum C_l/C_d compared with maximum C_l/C_d of its initial sampling at sampling number 8 is 2.08%. Figure 9 represents an example of initial sampling airfoil shape (sampling number 8) and optimized maximum C_l/C_d airfoil shape (sampling number 17).
The result in term of NACA-4 digit design variables:

- Percent of maximum camber is 4.33% of chord length.
- Percent of maximum camber position is 33.49% of chord length.
- Percent of maximum airfoil thickness is 5.08% of chord length.

The optimal airfoil shape can be written as NACA 4305 for sampling number 17.

Table 1 – C_l/C_d data for each airfoil sampling

Sampling Number	AoA (Degree)	C_l	C_d	C_l/C_d	
1	0.298949	0.5	0.012026	41.577152	Initial Sampling
2	4.459174	0.5	0.013170	37.964314	
3	1.138359	0.5	0.012355	40.468320	
4	1.735795	0.5	0.010822	46.202022	
5	2.320809	0.5	0.013073	38.245968	
6	1.122159	0.5	0.011850	42.195507	
7	1.137866	0.5	0.011045	45.269603	
8	0.034318	0.5	0.010814	46.237073	
9	0.570750	0.5	0.012301	40.648612	
10	1.682119	0.5	0.011931	41.907643	
11	0.682811	0.5	0.010815	46.231721	Iteration 1
12	0.563810	0.5	0.010751	46.507499	
13	0.399619	0.5	0.010873	45.987061	Iteration 2
14	0.388202	0.5	0.010867	46.009433	
15	0.663188	0.5	0.010639	46.998930	Iteration 3
16	2.102273	0.5	0.010662	46.893715	
17	0.553333	0.5	0.010594	47.198504	Iteration 4
18	0.467619	0.5	0.010607	47.139892	
19	0.915640	0.5	0.010650	46.947706	Iteration 5
20	0.821632	0.5	0.010707	46.697346	

The C_l/C_d results of the optimization process in Table 1 can be shown in the Figure 7.

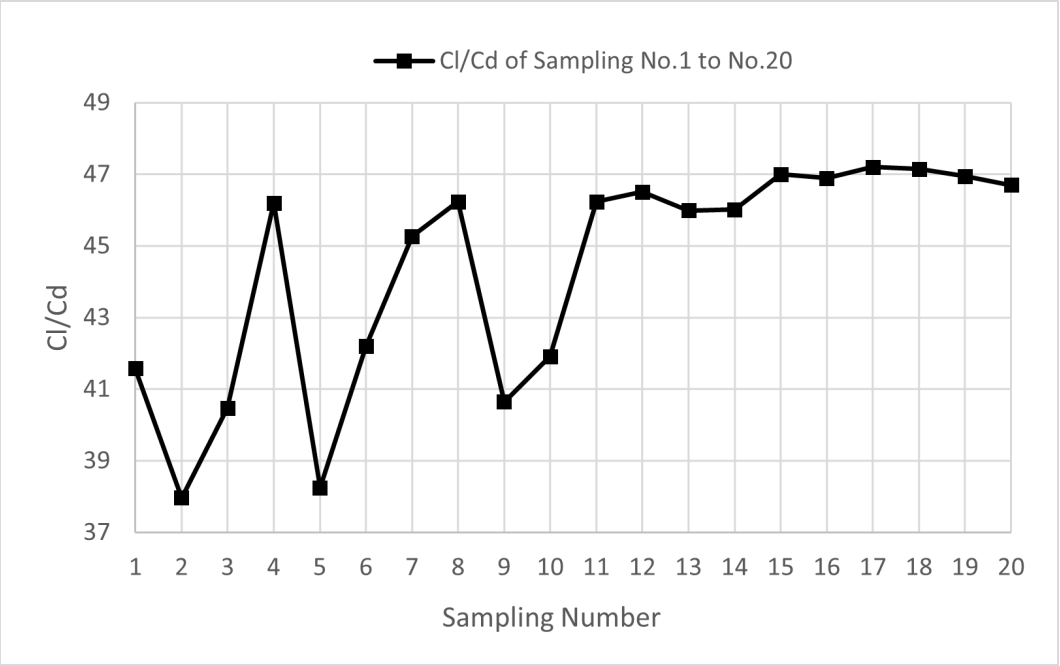

Figure 7 – C_l/C_d convergence for all sampling.

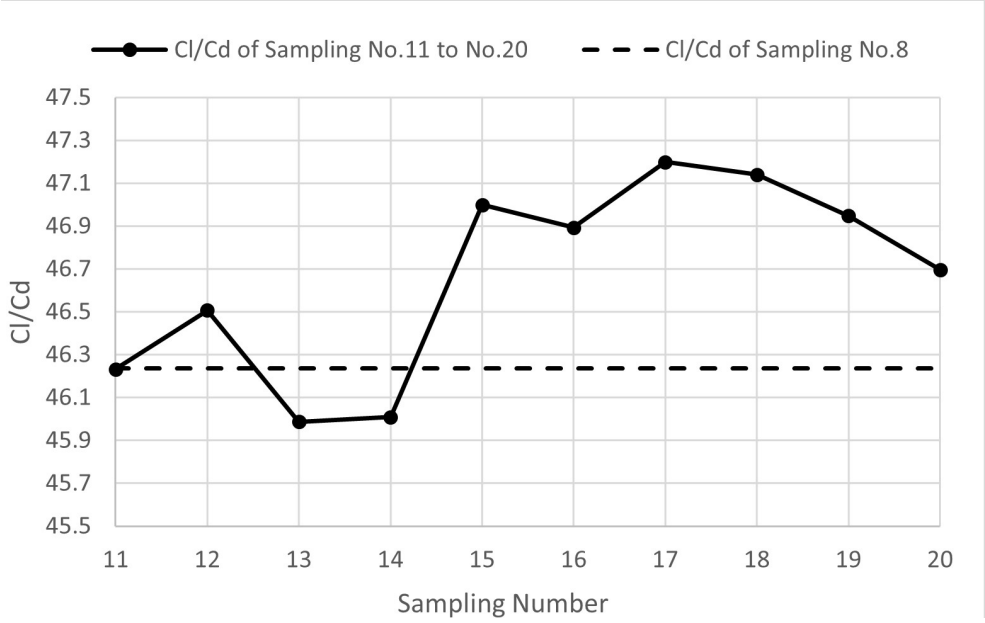

Figure 8 – C_l/C_d in each additional sampling from 5 iterations compared with the maximum C_l/C_d of initial sampling (Number 8, Dashed line).

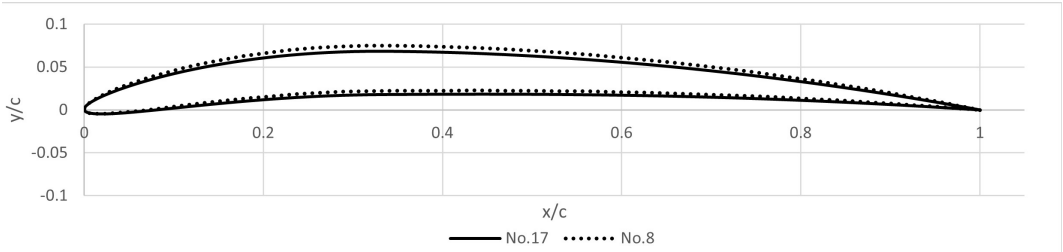

Figure 9 – Airfoil shape comparing between initial sampling (Number 8, Dotted line) and maximum C_l/C_d sampling (Number 17, Solid line).

4.2 Discussion

According to the results from the optimization process, Table 1 demonstrates the results of C_l/C_d for all sampling. From the additional sampling number, 11 to 20 represent the optimal range C_l/C_d is between 45.9871 to 47.1985. Figure 7 illustrates the C_l/C_d convergence value for all sampling in the optimization process. This result shows that the multi-additional sampling multi-fidelity EGO is applicable to finding the optimal airfoil design. Figure 9 represents the optimal airfoil shape, the result shows a comparison of the shape between initial sampling (Number 8) and additional sampling (Number 17) is a slightly different shape.

5. Conclusion

This paper studied applying Efficient Global Optimization (EGO) with parallel computing multi-additional sampling multi-fidelity for a single objective, this method can apply to finding the optimal NACA 4-digit airfoil design at maximum C_l/C_d at C_l = 0.5 with operating at Reynolds number at 1,000,000.
The development of the proposed method was achieved by incorporating sub-iterations to obtain multiple additional samples that can be used to improve the surrogate model.
The result in Figure 9 shows that the optimum shape design geometry is NACA 4305. The shape can be decreased slightly from its initial sampling shape at number 8 and the maximum C_l/C_d is approximately 47.20 at an approximate 0.55 degree of angle of attack with a 2.08% improvement compared with the maximum C_l/C_d of initial samplings.

6. Contact Author Email Address

Krittin Khankwa, Student, krittin.khankwa98@gmail.com
Atthaphon Ariyarit, Advisor, ariyarit@sut.ac.th

7. Copyright Statement

References

[1] Atthaphon Ariyarit and Masahiro Kanazaki. Multi-modal distribution crossover method based on two crossing segments bounded by selected parents applied to multi-objective design optimization. *Journal of Mechanical Science and Technology*, 29(4):1443–1448, 2015.

[2] Atthaphon Ariyarit, Tharathep Phiboon, Masahiro Kanazaki, and Sujin Bureerat. The effect of multi-additional sampling for multi-fidelity efficient global optimization. *Symmetry*, 12(9):1499, 2020.

[3] Mark Drela. Xfoil: An analysis and design system for low reynolds number airfoils. In *Low Reynolds number aerodynamics*, pages 1–12. Springer, 1989.

[4] Snorri Gudmundsson. Chapter 8 - the anatomy of the airfoil. In Snorri Gudmundsson, editor, *General Aviation Aircraft Design*, pages 235–297. Butterworth-Heinemann, Boston, 2014.

[5] Bart GM Husslage, Gijs Rennen, Edwin R Van Dam, and Dick Den Hertog. Space-filling latin hypercube designs for computer experiments. *Optimization and Engineering*, 12(4):611–630, 2011.

[6] Donald R Jones, Matthias Schonlau, and William J Welch. Efficient global optimization of expensive black-box functions. *Journal of Global optimization*, 13(4):455–492, 1998.

[7] Masahiro Kanazaki, Taro Imamura, Takashi Matsuno, and Kazuhisa Chiba. Multiple additional sampling by expected improvement maximization in efficient global optimization for real-world design problems. In *Intelligent and Evolutionary Systems*, pages 183–194. Springer, 2017.

[8] Georges Matheron. Principles of geostatistics. *Economic geology*, 58(8):1246–1266, 1963.

[9] Tharathep Phiboon, Atthaphon Ariyarit, Masahiro Kanazaki, Yuki Kishi, Sujin Bureerat, and Wannida Sae-Tang. Multi-additional sampling multi-objective efficient global optimization applied to uavs airfoil design problem. In *2021 18th International Conference on Electrical Engineering/Electronics, Computer, Telecommunications and Information Technology (ECTI-CON)*, pages 896–899. IEEE, 2021.

[10] R E Sheldahl and P C Klimas. Aerodynamic characteristics of seven symmetrical airfoil sections through 180-degree angle of attack for use in aerodynamic analysis of vertical axis wind turbines.

[11] Philippe Spalart and Steven Allmaras. A one-equation turbulence model for aerodynamic flows. In *30th aerospace sciences meeting and exhibit*, page 439, 1992.